The 2025 World Congress on
Advances in Structural Engineering and Mechanics (ASEM25)
BEXCO, Busan, Korea, August 11-14, 2025

A DEM study on critical state behaviour and stress-dilatancy of sand under constant stress increment ratio compression

*Wenlin Fu[1)], Guobin Gong[2)], Emma Michie[3)], Kang Chen[4)]

[1), 2), 4)] *Department of Civil Engineering, Xi'an Jiaotong-Liverpool Universit, P.R. China, Suzhou, Jiangsu, China*
[1), 3)] *Department of Earth, Ocean and Ecological Sciences, University of Liverpool, Liverpool, UK*
[1)] wenlin.fu19@student.xjtlu.edu.cn

ABSTRACT

The paper presents the investigation of the critical state and stress-dilatancy behaviour of both dense and loose sand under constant stress increment ratio compression tests via three-dimensional DEM (Discrete Element Method) simulations. The critical state is examined in terms of both macroscopic and microscopic responses, and the critical state lines are shown to be unique and independent of the stress path, initial confining pressure, and initial void ratio. For each initial confining pressure, the stress-dilatancy curves (dilation angle against mobilized friction angle) show dependency of the stress path and initial density state in the early shearing stages, but eventually converge together and form a common evolving trend in the late shearing stages. Bolton's empirical equation is found to match this common evolving trend.

1. INTRODUCTION

Soils are state-dependent materials, with their strength and volume-change behaviour influenced by factors such as stress path, density, and stress state. The Critical State Soil Mechanics (CSSM), proposed by Roscoe et al. (1958) and Schofield and Wroth (1968), unifies soil strength and volume change into one framework to explore soil's full stress-strain behaviour. Central to CSSM is the concept of critical state (CS), a condition achieved when soil is sheared to a certain strain level, where both the stress state and volume remain unchanged. Although the framework was initially developed for clay, later studies have shown that the behaviour of sand also fits well in CSSM, thereby extending the applicability of CSSM to sand (Wroth and Bassett 1965, Atkinson and Bransby 1978). Within the CSSM framework, a unique critical state line (CSL) is assumed to exist for a given type of soil, representing the soil's ultimate state.

The volume-change behaviour of soil towards CS is a central issue in studying the shear behaviour of granular materials (Reynold 1885, Bolton 1986). In modern soil

mechanics, 'dilatancy' is an alternative term referring to the volume change (either expansion or contraction) induced by shearing (Jefferies and Been 2015). Following Taylor's (1948) pioneering work, establishing the relationship between stress and dilatancy has been extensively explored by researchers (Rowe 1962, Roscoe et al. 1963, Roscoe and Burland 1968). Bolton (1986, 1987) proposed an empirical linear equation to describe the stress-dilatancy relation in terms of friction and dilation angles, as: $\psi = (\phi' - \phi'_c)/\alpha$, where ψ is the dilation angle, ϕ' is the mobilized friction angle, ϕ'_c is the CS friction angle, and α is the statistical constant coefficient.

This study investigates the CS behaviour and stress-dilatancy relationship of both dense and loose sand under constant stress increment ratio compression tests with different stress paths and initial confining pressures through 3D DEM. All samples are sheared to reach the CS, and both macroscopic and microscopic responses are analyzed. The stress-dilatancy relationship in terms of dilation angle and mobilized friction angle is demonstrated, and Bolton's empirical equation is examined.

2. SIMULATION DETAILS

2.1 Model Characteristic

The Discrete Element Method (DEM), originally developed by Cundall and Strack (1979), is a promising numerical technique for exploring both the macroscopic and microscopic behaviour of granular materials. In this study, the commercial program, three-dimensional Particle Flow Code (PFC 3D) version 6.0, developed by Itasca Consulting Group (2019), is used to conduct the numerical simulations of the constant stress increment ratio compression tests. For each time step, Newton's second law is applied to particles to determine the motion of each particle from the contact and body forces. Then, the force-displacement contact law is applied to contacts to update the contact forces from relative motion at each contact. The original particle assembly is created by initially generating non-contacting spheres in a cubic box with dimensions of 7.5 mm × 7.5 mm × 7.5 mm in 3D space, as shown in Fig. 1. The assembly contains 17505 particles in total, with particle diameters ranging from 0.1 mm to 1 mm. Fig. 2 depicts the sample's grain size distribution, which has a similar gradation to Hostun sand, a quartz sand frequently used in laboratory studies (Goudarzy et al. 2022).

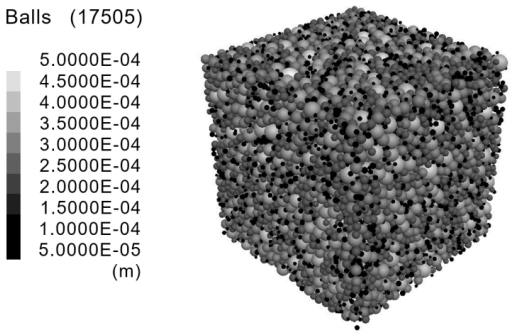

Fig. 1 Initial sample in PFC 3D

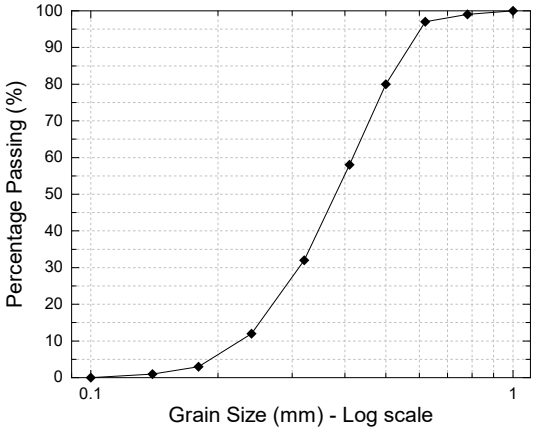

Fig. 2 Grain size distribution

The particles are then brought into contact through isotropic compression using servo-control until the sample reaches the targeted initial confining pressure (p_0'), with a maximum tolerance of $\pm$0.1%. Different p_0' in this study include 300 kPa and 500 kPa. The sand samples involve two different initial density states: dense and loose, which are achieved by setting a small or a large initial inter-particle friction coefficient (μ_i), while the wall friction coefficient (μ_w) always remains at zero throughout all stages. Table 1 lists the information on samples just after the isotropic compression, where the subsequent shearing will then start. Both the contacts between particle-to-particle and particle-to-wall adopt the linear contact model, which is effective for the simulation of non-cohesive granular materials (Di Renzo and Di Maio 2004). The input parameters and model properties used in the simulations are listed in Table 2. No gravitational field is applied.

Table 1. Initial states of samples after isotropic compression

Initial density state	Initial confining pressure	Initial void ratio
Dense	300	0.498
	500	0.481
Loose	300	0.613
	500	0.594

Table 2. Input parameters in DEM simulations

Input parameter	Value	Unit
Particle density ρ	2650	kg/m^3
Effective modulus E_e	1×10^8	Pa
Normal to shear stiffness ratio k_n/k_s	1.3	-
Contact damping factor ξ	0.3	-
Interparticle friction coefficient μ_p	0.35	-
Wall-particle friction coefficient μ_w	0	-

2.2 Stress Paths

A constant stress increment ratio test refers to the value of dq/dp' remains at a fixed value throughout the shearing process. In this study, after isotropically compressing to p_0', each sample then follows three different stress paths, specifically $dq/dp' = 2,\ 3,$ and 4, as illustrated in Fig. 3. Servo-control is used to achieve these stress paths with specific slope values of dq/dp', see Eq. (1) and Eq. (2). All simulations are terminated when the deviatoric strain (ε_d) reaches 40%, where the CS behaviour can be effectively captured.

$$\Delta\sigma_3' = \frac{3 - dq/dp'}{2 \cdot dq/dp' + 3} \cdot \Delta\sigma_1' \tag{1}$$

$$\sigma_3' = p_0' + \Delta\sigma_3' \tag{2}$$

In this paper, samples are denoted by codes representing their initial density state and stress path. For example, 'D/2' refers to the dense sample under a stress path with $dq/dp' = 2$; 'L/3' refers to the loose sample under a stress path with $dq/dp' = 3$.

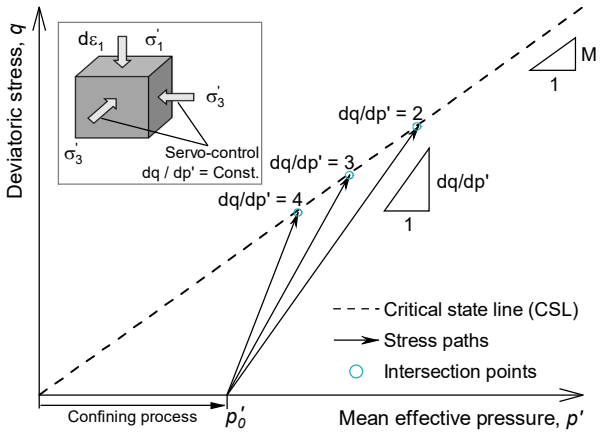

Fig. 3 Stress paths under constant stress increment ratio compression

3. RESULTS AND DISCUSSION

3.1 Evolution of Macroscopic behavior

Figs. 4 (a, b) show the evolutions of deviatoric stress (q) against deviatoric strain (ε_d) for samples with different p_0'. It is observed that each dense sample initially exhibits strain hardening until reaching a peak value, followed by strain softening until a plateau is reached at CS. In contrast, loose samples exhibit only strain hardening, with q progressively rising to the CS values.

Figs. 5 (a, b) show the evolutions of mean effective pressure (p') against deviatoric strain (ε_d) for samples with different p_0'. It is observed that the evolution trends of p' show similarities with the evolutions of q, that dense samples initially rise to the peak values before decreasing to the CS, while loose samples gradually increase towards the CS.

Figs. 6 (a, b) show the evolutions of void ratio (e) against deviatoric strain (ε_d) for samples with different p_0'. It is observed that the volume change (or dilatancy) of dense samples exhibits an initial contraction (i.e., initial decrease in e) before transitioning to dilation (i.e., increase in e), while loose samples consistently exhibit contraction until reaching CS.

Overall, for each same p_0', the CS values of q, p', and e are found to depend on the stress path, but are otherwise unique and independent of the initial density state (i.e., dense or loose). As the value of dq/dp' increases, the CS values of q and p' are found to increase accordingly, while the CS values of e are found to decrease accordingly. For samples under a given stress path, a higher p_0' leads to higher CS values of q and p', and lower CS values of e.

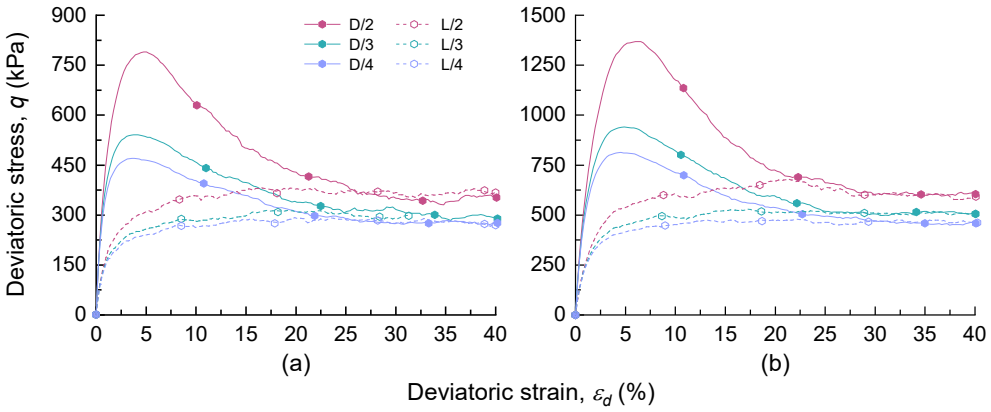

Fig. 4 Evolutions of deviatoric stress (q) under constant stress increment ratio compression with initial confining pressures (p_0') of: (a) 300 kPa; (b) 500 kPa

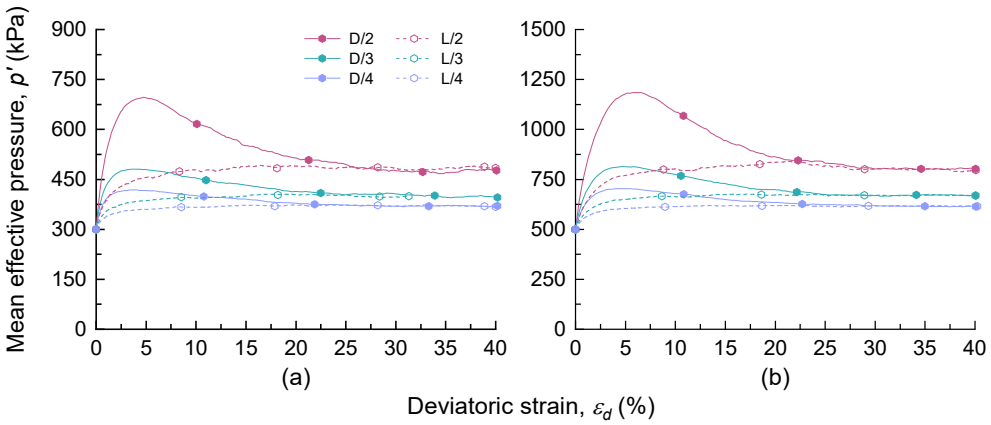

Fig. 5 Evolutions of mean effective pressure (p') under constant stress increment ratio compression with initial confining pressures (p_0') of: (a) 300 kPa; (b) 500 kPa

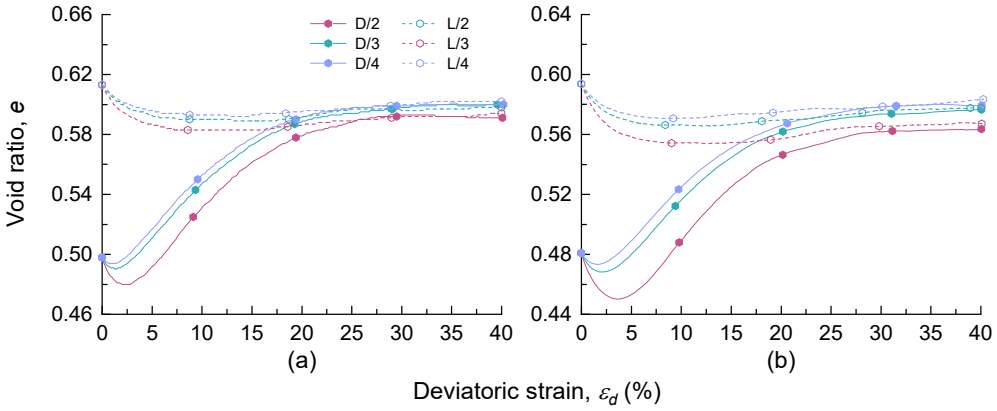

Fig. 6 Evolutions of void ratio (e) under constant stress increment ratio compression with initial confining pressures (p_0') of: (a) 300 kPa; (b) 500 kPa

3.2 Evolution of Microscopic behavior

The average/apparent coordination number (Z) describes the average number of contacts per particle (i.e., contact density), as given by:

$$Z = \frac{2C}{N_t} \tag{3}$$

where C refers to the total number of contacts and N_t refers to the number of particles in the system. However, particles with one or no contact do not contribute to the system stability, and, thereby, should be excluded. Therefore, the mechanical coordination number (Z_m) is adopted by researchers (Thornton 2000, Gong and Zha 2013), as given by:

$$Z_m = \frac{2C - N_1}{N_t - N_0 - N_1} \tag{4}$$

where N_1 and N_0 are the numbers of particles with one and no contact, respectively.

Figs. 7 (a, b) show the evolutions of mechanical coordination number (Z_m) against deviatoric strain (ε_d) for samples with different p_0'. It is observed that for each same p_0', the CS values of Z_m are found to depend on the stress path, but are otherwise unique and independent of the initial density state (i.e., dense or loose). As the value of dq/dp' increases, the CS values of Z_m are found to increase accordingly. By comparing the sub-figures, it can be seen that the increase in p_0' leads to higher initial values of Z_m, reflecting a higher contact density between particles under a higher p_0'. In addition, for samples under a given stress path, a higher p_0' leads to higher CS values of Z_m.

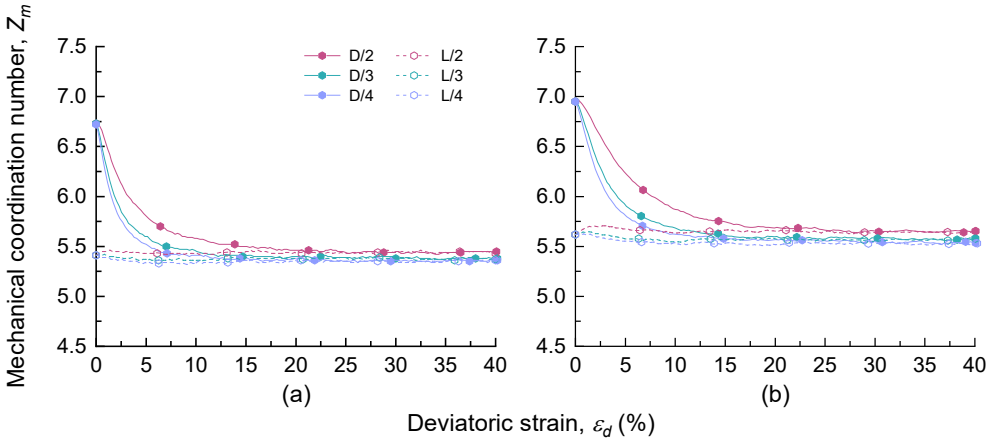

Fig. 7 Evolutions of mechanical coordination number (Z_m) under constant stress increment ratio compression with initial confining pressures (p_0') of: (a) 300 kPa; (b) 500 kPa

3.3 Critical State Analysis

The CS values represent soil's ultimate state, and are determined as the mean values over the last 10% ε_d. A set of CS values for macroscopic responses (e, q, and p') and microscopic responses (Z and Z_m) are obtained for all samples, and the CSLs are plotted in Figs. 8 (a, b, c) and Figs. 9 (a, b). In the classical CSSM framework, the CSLs in $e - q - p'$ space can be projected onto $q - p'$ and $e - lg(p')$ planes. However, for cohesionless soils such as sand, the CSLs are generally nonlinear in $e - lg(p')$ plane, as shown in Fig. 8 (a). In order to better describe the relationship between the CS void ratio (e_{cs}) and CS mean effective pressure (p_{cs}') for cohesionless soils, Li and Wang (1998) proposed a method to linearize the CSL in $e - (p'/p_a)^{\beta}$ plane, as given by:

$$e_{cs} = \Gamma - \lambda \left(\frac{p_{cs}'}{p_a}\right)^{\beta} \tag{5}$$

where Γ is the intercept of the CSL when $p'_{cs} = 0$, λ is the absolute value of the slope, p_a is the atmosphere pressure (101.325 kPa), β is the statistical constant coefficient. In this study, the best-fit value of β is 0.954, see Fig. 8 (b), in which an apparently unique CSL can be observed. The CSL in $q - p'$ plane is shown in Fig. 8 (c), which is a straight line that passes through the origin with a slope of the CS stress ratio (M) equal to 0.748. For a given type of sand under compression, the value of M is unique, reflecting an intrinsic characteristic of the soil.

Fig. 9 (a) shows the CSLs of CS average coordination number (Z_{cs}) and CS mechanical coordination number ($Z_{m,cs}$) against p'_{cs}. It can be seen that both Z_{cs} and $Z_{m,cs}$ show an increasing tendency with rising p'_{cs}, which can be attributed to the increasing interparticle contacts. It is also observed that as p'_{cs} increases, the gap between Z_{cs} and $Z_{m,cs}$ gradually narrows. Fig. 9 (b) shows the CSLs of Z_{cs} and $Z_{m,cs}$ against e_{cs}, which shows that as e_{cs} increases, both Z_{cs} and $Z_{m,cs}$ decrease, and the gap between Z_{cs} and $Z_{m,cs}$ widens. It is found that the CSLs of $Z_{cs} - p'_{cs}$, $Z_{m,cs} - p'_{cs}$, $Z_{cs} - e_{cs}$, and $Z_{m,cs} - e_{cs}$ are all logarithm relationships, as shown in Figs. 9 (a, b). All CSLs show independency of the initial void ratio, p'_0, and stress path.

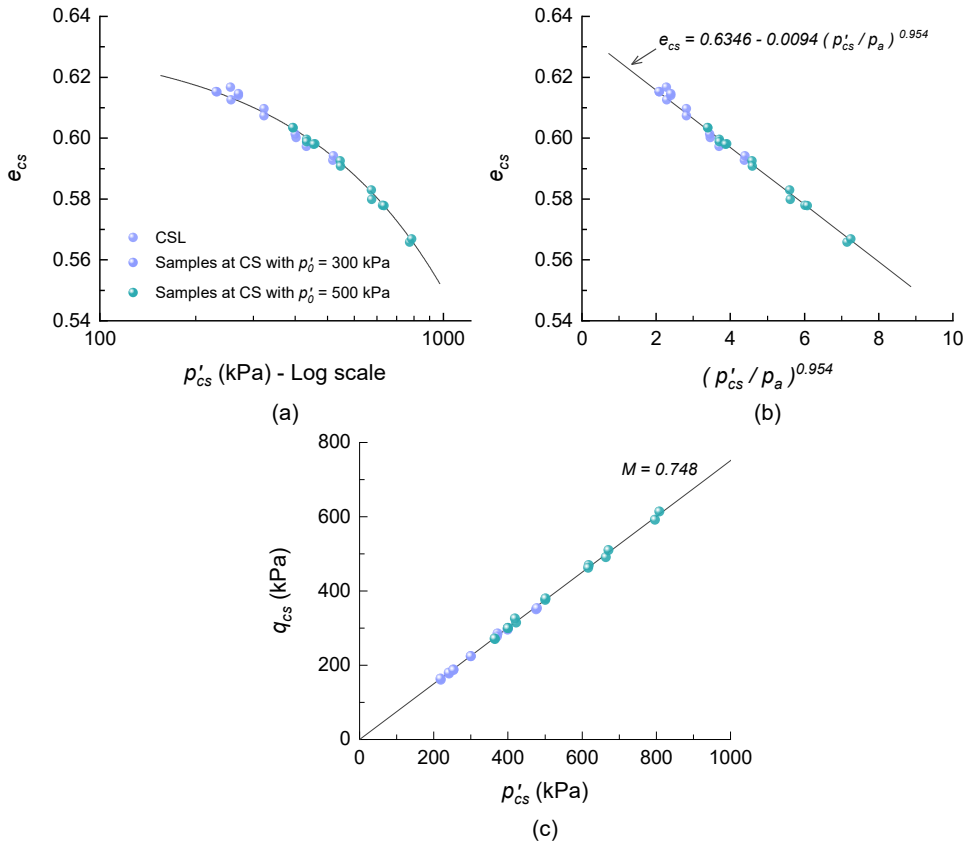

Fig. 8 CSL in the plane of (a) $e - lg(p')$; (b) $e - (p'/p_a)^{0.954}$; (c) $q - p'$

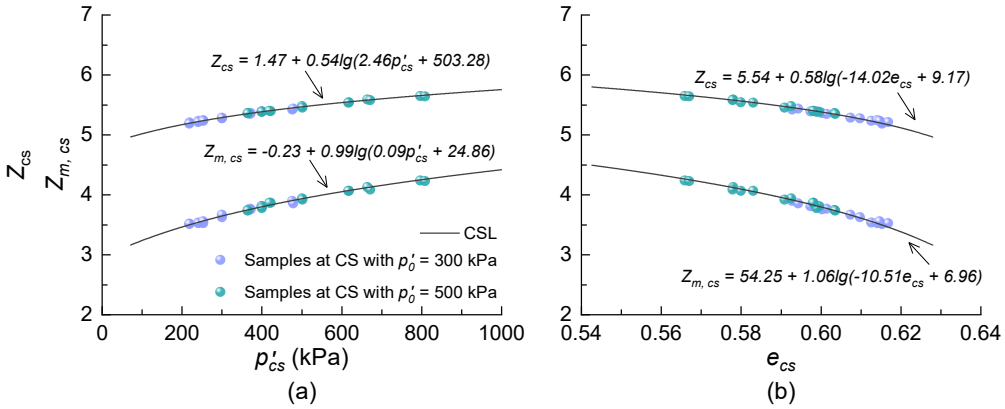

Fig. 9 CSLs in the plane of (a) $Z - p'$ and $Z_m - p'$; (b) $Z - e$ and $Z_m - e$

3.4 Stress-Dilatancy

The stress-dilatancy relationship can be described in terms of the correlation between dilation and friction angles. For axisymmetric compression conditions, the expression of dilation angle (ψ) is defined (Vermeer and de Borst 1984) as:

$$\psi = arcsin\ \frac{-d\varepsilon_v^p}{2d\varepsilon_1^p - d\varepsilon_v^p} \tag{6}$$

where $d\varepsilon_1^p$ is plastic axial strain increment and $d\varepsilon_v^p$ is plastic volumetric strain increment. A positive ψ indicates dilation, while a negative ψ indicates contraction. According to elastoplastic theory, the difference between total strains and plastic strains can be neglected (Wood and Belkheir 1994, Li and Dafalias 2000, Hanley et al. 2018, Jin et al. 2022). Therefore, total strain increments (instead of plastic strain increments) are used in Eq. (6) in this study.

The definition of friction angle is based on the Mohr-Coulomb strength criterion. The mobilized friction angle (ϕ') is expressed as:

$$\phi' = arcsin\ \frac{\sigma_1' - \sigma_3'}{\sigma_1' + \sigma_3'} \tag{7}$$

where σ_1' and σ_3' are the major and minor principal effective stresses, respectively.

Figs. 10 (a, b) and Figs. 11 (a, b) show the evolutions of dilation angle (ψ) and mobilized friction angle (ϕ') against deviatoric strain (ε_d) under constant stress increment ratio compression for dense and loose samples, respectively. It is observed that the initial slopes of ψ vary for different stress paths, that a higher value of dq/dp' leads to a steeper initial slope of ψ. During evolution, dense samples exhibit obvious peak values of ψ, while loose samples do not. Ultimately, all evolution curves of ψ reach a plateau

at zero, indicating no more volume change at CS. The evolution curves of ϕ' for dense samples exhibit obvious peak values, while loose samples do not. However, all curves of ϕ' ultimately reach a plateau at the same CS value $\phi'_c = 19.47°$, which is independent of stress path, p'_0, and initial void ratio, indicating that ϕ'_c is an intrinsic mechanical property for a given soil.

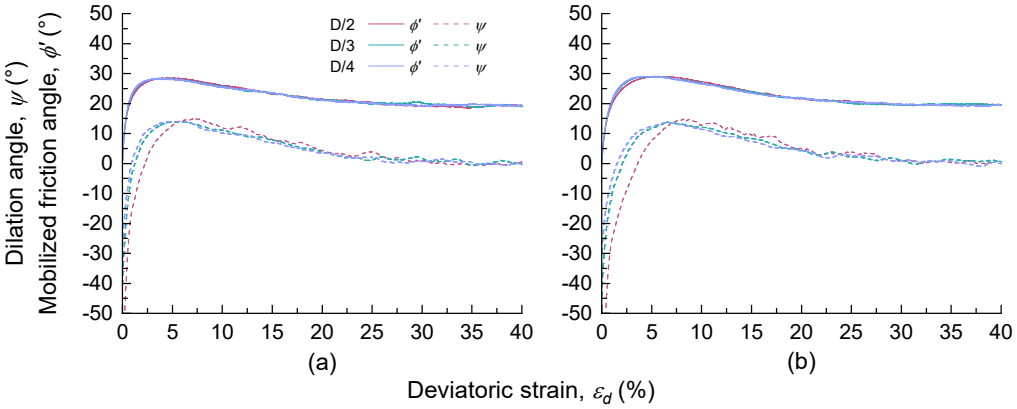

Fig. 10 Evolutions of mobilized friction angle (ϕ') and dilation angle (ψ) for dense samples under constant stress increment ratio compression with initial confining pressures (p'_0) of: (a) 300 kPa; (b) 500 kPa

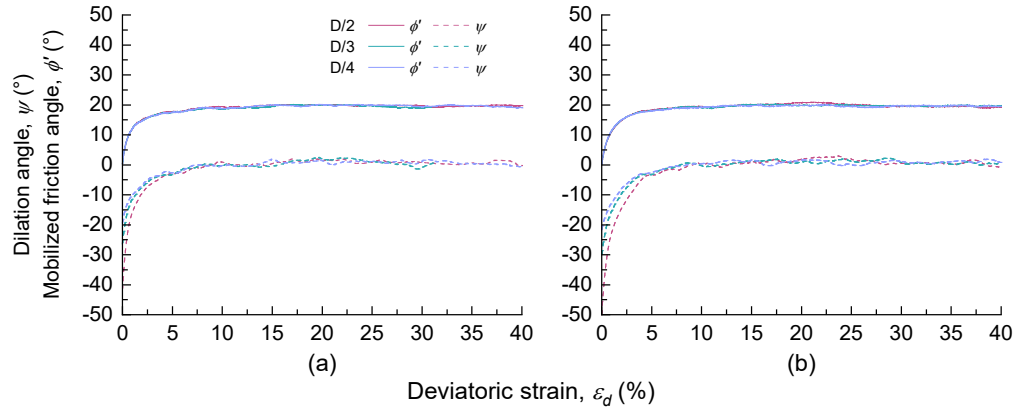

Fig. 11 Evolutions of mobilized friction angle (ϕ') and dilation angle (ψ) for loose samples under constant stress increment ratio compression with initial confining pressures (p'_0) of: (a) 300 kPa; (b) 500 kPa

Figs. 12 (a, b) show plots of ψ against ϕ' for both dense and loose samples with different p'_0 under constant stress increment ratio compression. For each p'_0, it is observed that different stress paths and initial density states are found to induce different $\psi - \phi'$ curves in the initial shearing stages. Dense samples are observed to exhibit a 'turning hook' around the peak ϕ', after which all the $\psi - \phi'$ curves for dense samples

converge together, forming a common evolving trend, and eventually settle at CS, where $\psi = 0$ and ϕ' is approximately 19.47°. Loose samples do not exhibit a 'turning hook' but the $\psi - \phi'$ curves gradually converge to the same common evolving trend as dense samples and settle at CS. It is found that this common evolving trend can be described using Bolton's empirical equation, as shown in Figs. 12 (a, b), where the best-fit value of the coefficient α is found to be independent of the stress path and initial void ratio but vary with different p_0'.

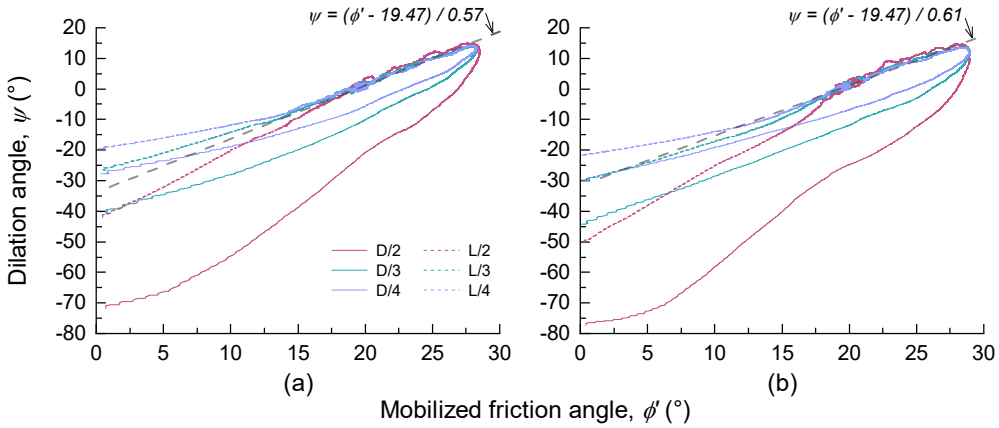

Fig. 12 Dilation angle (ψ) against mobilized friction angle (ϕ') under constant stress increment ratio compression with initial confining pressures (p_0') of: (a) 300 kPa; (b) 500 kPa

4. CONCLUSION

In this study, the critical state (CS) behaviour and stress-dilatancy relationship of dense and loose sand are investigated via DEM simulations of constant stress increment ratio compression tests. The CS behaviour is discussed for both macroscopic and microscopic responses. The dilatancy is investigated in terms of the dilation angle. Based on the results, the main conclusions are as follows:

- With the same p_0', the CS values of q, p', Z_m, and e are found to depend on stress path, but are otherwise unique and independent of the initial density state. For samples under a given stress path, the increase in p_0' leads to higher CS values of q, p', and Z_m, and lower CS values of e. The CSLs are examined to be unique and independent of stress path, p_0', and initial void ratio.

- With the same p_0', samples show different $\psi - \phi'$ curves due to different stress paths and initial density states in the initial shearing stages. However, all curves eventually converge together, forming a 'common evolving trend' in the late shearing stages, and settle at CS. Bolton's empirical equation: $\psi = (\phi' - \phi_c')/\alpha$ is found to match this 'common evolving trend' in the late shearing stages. The value of coefficient α is found to vary for different p_0'.

REFERENCES

Atkinson, J. H. and Bransby, P. (1978), *The mechanics of soils: an introduction to critical state soil mechanics*, McGraw Hill, London.

Bolton, M. (1986), "The strength and dilatancy of sands", *Géotechnique*, Vol. **36**(1), 65-78.

Bolton, M. (1987), Discussion: The strength and dilatancy of sands. *Géotechnique*, Vol. **37**(2), 219-226.

Cundall, P. A. and Strack, O. D. (1979), "A discrete numerical model for granular assemblies", *Géotechnique*, Vol. **29**(1), 47-65.

Di Renzo, A. and Di Maio, F. P. (2004), "Comparison of contact-force models for the simulation of collisions in DEM-based granular flow codes", *Chem. Eng. Sci.*, Vol. **59**(3), 525-541.

Gong, G. and Zha, X. (2013), "DEM simulation of undrained behaviour with preshearing history for saturated granular media", *Model. Simul. Mater. Sci. Eng.*, Vol. **21**(2), 025001.

Goudarzy, M., Sarkar, D., Lieske, W. and Wichtmann, T. (2022), "Influence of plastic fines content on the liquefaction susceptibility of sands: monotonic loading", *Acta Geotech.*, 1-19.

Hanley, K. J., Huang, X. and O'Sullivan, C. (2018), "Energy dissipation in soil samples during drained triaxial shearing", *Géotechnique*, Vol. **68**(5), 421-433.

Itasca (2019), *Particle flow code in 3 dimensions (PFC3D)*, Itasca Consulting Group Inc, Minneapolis, Minnesota, USA.

Jefferies, M. and Been, K. (2015), *Soil liquefaction: a critical state approach*, Taylor & Francis Group, New York.

Jin, W., Tao, Y. and Chen, R. (2022), "Capturing the Turning Hook of Stress-Dilatancy Curve of Crushable Calcareous Sand", *J. Mar. Sci. Eng.*, Vol. **10**(9), 1269.

Li, X. S. and Wang, Y. (1998), "Linear representation of steady-state line for sand", *J. Geotech. Geoenviron. Eng.*, Vol. **124**(12), 1215-1217.

Li, X. S. and Dafalias, Y. F. (2000), "Dilatancy for cohesionless soils", *Géotechnique*, Vol. **50**(4), 449-460.

Reynolds, O. (1885), "LVII. On the dilatancy of media composed of rigid particles in contact. With experimental illustrations", *Lond. Edinb. Dubl. Phil. Mag. J. Sci.*, Vol. **20**(127), 469-481.

Roscoe, K. H. and Burland, J. B. (1968), *On the generalized stress-strain behaviour of wet clay, In Engineering plasticity*, Cambridge University Press, London, 535-609.

Roscoe, K. H., Schofield, A. and Wroth, A. P. (1958), "On the yielding of soils", *Géotechnique*, Vol. **8**(1), 22-53.

Roscoe, K. H., Schofield, A. N. and Thurairajah, A. (1963), "Yielding of clays in states wetter than critical", *Géotechnique*, Vol. **13**(3), 211-240.

Rowe, P. W. (1962), "The stress-dilatancy relation for static equilibrium of an assembly of particles in contact", *Proc. R. Soc. Lond. A. Math. Phys. Sci.*, Vol. **269**(1339), 500-527.

Schofield, A. N. and Wroth, P. (1968), *Critical state soil mechanics*, McGraw Hill, London.

Taylor, D. W. (1948), *Fundamentals of soil mechanics*, Jon Wiley and Sons Inc., New York.

Thornton, C. (2000), “Numerical simulations of deviatoric shear deformation of granular media”, *Géotechnique*, Vol. **50**(1), 43-53.
Vermeer, P. A. and de Borst, R. (1984), “Non-associated plasticity for soils, concrete and rock”, *Heron*, Vol. **29**(3), 3-64.
Wood, D. M. and Belkheir, K. (1994), “Strain softening and state parameter for sand modelling”, *Géotechnique*, Vol. **44**(2), 335-339.
Wroth, C. and Bassett, R. (1965), “A stress–strain relationship for the shearing behaviour of a sand”, *Géotechnique*, Vol. **15**(1), 32-56.